PCCP

Accepted Manuscript

ROYAL SOCIETY OF CHEMISTRY

www.rsc.org/pccp

PCCP

RSCPublishing

COMMUNICATION

Role of Schottky barrier in the resistive switching of $SrTiO_3$: Direct experimental evidences

Cite this: DOI: 10.1039/xoxxoooooox

Xue-Bing Yin,[a] Zheng-Hua Tan[a] and Xin Guo[a]*

Received ooth January 2014,
Accepted ooth January 2014

DOI: 10.1039/xoxxoooooox

www.rsc.org/

Single crystalline $SrTiO_3$ doped with 0.1 wt.% Nb was used as a model system to evaluate the role of the Schottky barrier in the resistive switching of perovskites. The Ti bottom electrode formed an ohmic contact in the Ni/Nb:$SrTiO_3$/Ti stack, whereas the Ni top electrode created a strong Schottky barrier, which was reflected by a huge semi-circle in the impedance spectrum of the stack. Bipolar switching was achieved in the voltage range of –4 to 4 V for the stack, two clear resistance states were created by electric pulses, and the Schottky barrier heights corresponding to the high/low resistance states were experimentally determined. A direct relation between the resistance state and the Schottky barrier height was thus established.

The phenomenon of resistive switching has been extensively observed in various perovskite oxides, such as $Pr_{1-x}CaMnO_3$,[1] $SrZrO_3$,[2] $SrTiO_3$,[3] and $BaTi_{0.95}Co_{0.05}O_3$,[4] and $Pb(Zr_{0.2}Ti_{0.8})O_3$.[5] Among perovskite oxides, $SrTiO_3$ has been thoroughly investigated;[6-12] the knowledge about $SrTiO_3$ helps understanding the switching behaviours of other perovskite oxides. Therefore, $SrTiO_3$ is addressed in this work as a model system.

Quite different mechanisms have been proposed to explain the switching behaviours of $SrTiO_3$, and the most relevant switching mechanisms have been reviewed by Waser et al.[13,14] and Sawa.[15] Usually the works on acceptor- (e.g. Cr) doped $SrTiO_3$[6,9] emphasize the property change in the crystal bulk, in which, oxygen vacancies (or oxygen ions) play a key role: either the fast transport of oxygen vacancies along dislocations[10] or the formation of oxygen-vacancy array under high electrical stress[11] was suggested to be responsible for the switching. Guo[16] performed the electroforming of acceptor-doped $SrTiO_3$ single crystals at 200 ℃ and realized bipolar switching at room temperature. Since oxygen vacancies (or oxygen ions) are sufficiently mobile at 200 ℃, this work established a clear relation between the migration of oxygen vacancies and the resistive switching. In a very recent work,[17] the concentration variation of oxygen ions at different resistance states was directly measured.

A Schottky barrier is formed at the metallic electrode/$SrTiO_3$ contact, therefore, for donor- (e.g. Nb) doped $SrTiO_3$ the role of the Schottky barrier is emphasized:[7,8,14,15] the change in the Schottky barrier height under voltages of different polarities are responsible for the different resistance states. The important experimental evidences for the Schottky barrier model are:[15] (1) the on/off resistances of Nb-doped $SrTiO_3$ is inversely proportional to the electrode/$SrTiO_3$ interface area, suggesting that the resistive switching takes place over the entire interface area, and (2) Nb-doped $SrTiO_3$ with ohmic contact does not show any switching behaviour; whereas, Nb-doped $SrTiO_3$ with Schottky-type contact shows the resistive switching, and the switching behaviour can be alternated by modifying the electrode/$SrTiO_3$ interface.

However, the effect of the Schottky barrier was not separated from that of the bulk of donor-doped $SrTiO_3$ in many cases. For example, the stack (interface plus bulk) capacitance was measured without differentiating the contribution of the crystal bulk from that of the interface;[18] as a result, one could not conclude that the different capacitances in the low and high resistance states were only due to the interface effect. Also the direct link between the Schottky barrier height and the resistance state is still lacking.

An obvious advantage of the impedance spectroscopy technique is that the interface effect and the bulk contribution can be readily separated.[19] Impedance spectroscopy has been popularly used to investigate the switching of Fe-doped $SrTiO_3$,[19] Nb-doped $SrTiO_3$,[20] $(Ba,Sr)(Zr,Ti)O_3$,[21] NiO and TiO_2,[22] $SrZrO_3$,[23] and graphene oxide;[24] in most of these cases, the impedance spectroscopy was used to characterize the bulk properties of thin films, and in all the cases, the Schottky barrier height was not determined.

In this work, the impedance responses of the Schottky barrier in the high resistance state (HRS) and the low resistance state (LRS) were measured, and the bias-dependent response of the Schottky barrier unambiguously demonstrated that one could change the stack

resistance by orders of magnitude only by manipulating the Schottky barrier height. More important, the Schottky barrier heights of HRS and LRS were derived from the *I-V* and $1/C^2$-*V* curves, and a direct relation between HRS/LRS and a larger/smaller barrier height was established.

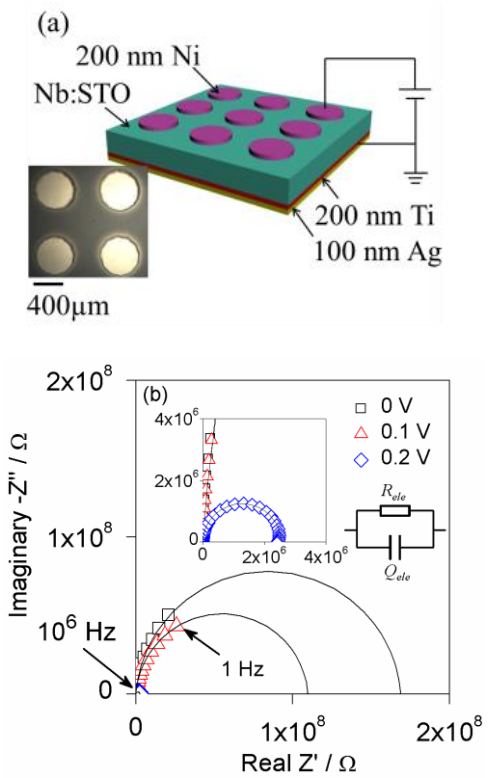

Fig. 1 (a) Configuration of Ni/Nb:$SrTiO_3$/Ti stack, and the inset is the optical image of the top Ni electrodes, and (b) bias-dependence of Ni/Nb:$SrTiO_3$/Ti stack. Insets (upper) are magnified impedance spectrum under 0.2 V bias (left), and equivalent circuit for fitting the impedance spectrum (right).

Ni/Nb:$SrTiO_3$/Ti stacks were fabricated in this work. The sample configuration is illustrated in Fig. 1(a). (100)-oriented $SrTiO_3$ single crystals ($5\times5\times0.5$ mm^3) doped with 0.1 wt. % Nb (CrysTec, Germany) were used. Top Ni electrode (diameter: 0.4 mm, thickness: 200 nm) and bottom Ti electrode (area: 5×5 mm^2, thickness: 200 nm) were prepared by sputtering with shadow masks. The Ti electrode was further capped with 100 nm thick Ag layer to prevent oxidation.

Nb-doped $SrTiO_3$ (Nb:$SrTiO_3$) is a *n*-type semiconductor with a wide band gap of 3.3 eV,[25] and a Ti electrode usually forms an ohmic contact at the Ti/Nb:$SrTiO_3$ junction.[26] However, owing to the large work function of Ni (ϕ_M=5.15 eV), a Ni electrode forms a Schottky barrier at the Ni/Nb:$SrTiO_3$ junction; a Schottky barrier composes of a depletion layer of electrons at the Ni/Nb:$SrTiO_3$ interface. According to the Schottky-Mott relation:[27] $\phi_B = \phi_M - \chi_S$ (where χ_S is the electron affinity, ~3.9 eV for $SrTiO_3$ (Ref. 25)), the ideal Schottky barrier height ϕ_B for the Ni/Nb:$SrTiO_3$ junction is ~1.25 eV.

The properties of the Nb:$SrTiO_3$ single crystal and the Schottky barrier at the Ni/Nb:$SrTiO_3$ junction can be separated by the impedance spectroscopy, and the impedance spectroscopy investigations were carried out with a 1260 Frequency Response Analyzer, in conjunction with a 1296 Dielectric Interface (Solartron Instruments, Farnborough, U.K.) in the frequency range of 1 to 10^6 Hz at an amplitude of 50 mV in air and at ambient temperature. Fig. 1(b) shows the impedance spectra of the Ni/Nb:$SrTiO_3$/Ti stack under different dc bias voltages; all the spectra are characterized by semi-circles. The bulk resistance of the Nb:$SrTiO_3$ single crystal was measured to be ~170 Ω, while the resistance of the Ni/Nb:$SrTiO_3$/Ti stack, as determined from the intersect of the impedance semi-circle on the real axis, was ~1.68×10^8 Ω under 0 V bias; therefore, the huge semi-circle can only be due to the impedance response of the Schottky barrier. Very interestingly, the semi-circle could be depressed by applying dc biases, as shown in Fig. 1(b). Such a phenomenon further demonstrates that the semi-circle is due to the Schottky barrier, because the bulk resistance of the Nb:$SrTiO_3$ single crystal could not be modified by the biases ≤ 0.2 V.

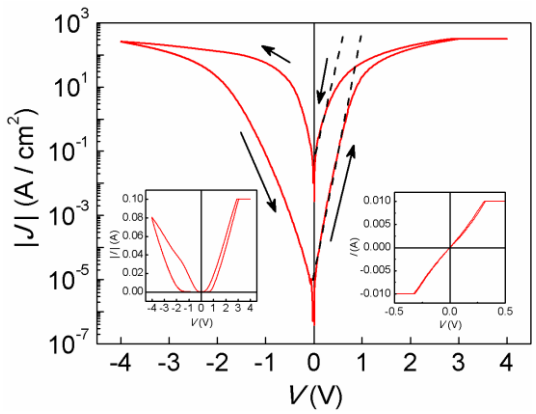

Fig. 2 Hysteric current density *J*- voltage *V* curve of Ni/Nb:$SrTiO_3$/Ti stack. The voltage sweeping was set to be 0 → +4 → 0 → –4 → 0 V. The left inset shows the corresponding *I-V* curve on linear scale, and the right one is the *I-V* curve of the Ti/Nb:$SrTiO_3$/Ti stack, demonstrating the ohmic contact between Ti and Nb:$SrTiO_3$.

The current *I*- voltage *V* characteristics of the Ni/Nb:$SrTiO_3$/Ti stack were investigated by the Keithley 4200 semiconductor characterization system in air and at the ambient temperature. The voltage sweep was set to be 0 → $+V_{max}$ → 0 → $-V_{max}$ → 0 V. The hysteretic semi-logarithmic current density *J*- voltage *V* curve is depicted in Fig. 2; the stack could be set from HRS to LRS by applying positive forward voltages, and reset from LRS back to HRS by applying negative reverse voltages. However, when Ti was applied for both the top and bottom electrodes, only ohmic contact was achieved, as evidenced by the right inset in Fig. 2.

HRS and LRS could also be created by applying electric pulses; a sequence of electric pulses with the amplitudes between –12 and +12 V and the width of 1 *ms* were applied to the Ni/Nb:$SrTiO_3$/Ti stack, and the stack resistance was recorded under a voltage of –0.1 V after each pulse. The results are given in Fig. 3(a). By applying pulses of +12, –12, –10, –8, –6 V, LRS with the resistance of ~10 KΩ and different HRSs with the resistances of ~1600, ~780, ~260, ~50 KΩ, were obtained. A relaxation of the resistance states could be

observed, which was especially noticeable for LRS. The variation of low resistance R with time is shown in Fig. 3(b), and it follows the Curie-Von Schweidler law $R \propto t^{\beta}$, here β is a constant less than 1. This equation describes charge trapping effect in high-κ dielectrics.[28] It was suggested that this resistance relaxation could be understood by the defects near the interface.[29]

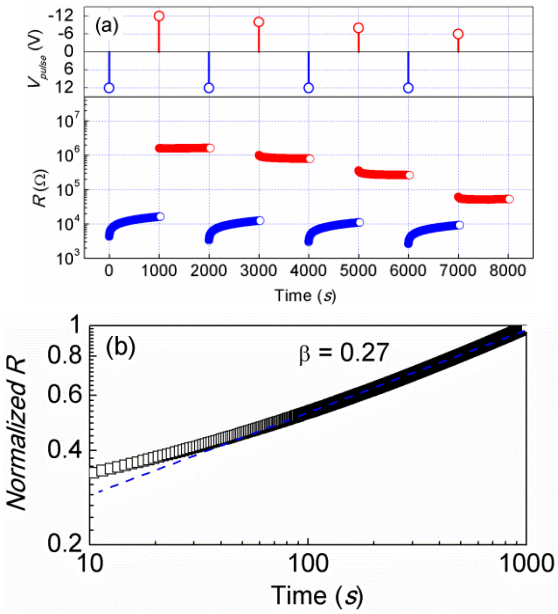

Fig. 3 (a) Pulses with amplitudes of +12，–12, –10, –8 and –6 V (upper) and corresponding resistance responses (lower). Pulse width was fixed at 1 *ms*. Read voltage was –0.1 V. (b) Relaxation of low resistance with time. $R_{Nomalized} = R / R_{Time=1000s}$.

To demonstrate the *I-V* characteristic more clearly, the *I-V* curve of the Ni/Nb:SrTiO$_3$/Ti stack is replotted on linear scale in Fig. 2 (the left inset). At room temperature, the thermal voltage ($V_T = k_BT/q$) is approximately 26 mV; when the applied voltage is higher than the thermal voltage, the current increases exponentially, and such behaviour can be described by Eq. (1),[27]

$$J = A^{**}T^2 exp(-\phi_B/k_BT) exp(qV/nk_BT) \quad (1)$$

where A^{**} is the effective Richardson constant (156 Acm^{-2}K^{-2} for Nb:SrTiO$_3$[30]), T the absolute temperature, k_B the Boltzmann constant, q the electron charge, ϕ_B the Schottky barrier height and n the ideality factor. The ideality factor n describes the deviation from the ideal thermionic emission. By fitting the linear log*J*-*V* sections in Fig. 2 according to Eq. (1), one can determine the n and $\phi_B$values; the Schottky barrier heights ϕ_B thus deduced are 0.72 eV for HRS and 0.50 eV for LRS, and the ideality factors n are 2.12 for HRS and 2.54 for LRS. The Schottky barrier height ϕ_B and ideality factor n of HRS deviating from the expected value (ϕ_B = 1.25eV and n = 1) could be attributed to the presence of the interface layer and/or interface states.[26,28]

To further understand the Ni/Nb:SrTiO$_3$ interface, the capacitance *C*- voltage *V* characteristic was measured at 1 MHz with a signal of 50 mV, and the $1/C^2$- *V* curves at HRS and LRS are given in Fig. 4.

The carbon contamination or the atomic rearrangement when a metal electrode is deposited on the SrTiO$_3$ surface causes an interface layer at the electrode/SrTiO$_3$ junction.[28,30] Taking the interfacial layer into consideration, the junction capacitance is described by [31]

$$\frac{1}{C^2} = \frac{2n[nV_{bi} - V - (nk_BT/q)]}{q\varepsilon_0\varepsilon_r N_d} \quad (2)$$

where V_{bi}, N_d, ε_0, ε_r are the built-in potential, dopant concentration, vacuum permittivity, and relative dielectric constant, respectively. Fitting the experimental results given in Fig. 4 according to Eq. (2), the built-in potentials were deduced to be 1.16 eV and 0.78 eV for HRS and LRS, respectively. For Nb:SrTiO$_3$, $V_{bi} - \phi_B \approx 0.1$ eV,[32] therefore, the Schottky barrier heights could thus be determined to be 1.06 eV and 0.68 eV for HRS and LRS, respectively. These values are larger than those deduced from the *J*- *V* fitting, but the Schottky barrier height at HRS is quite close to the ideal height value.

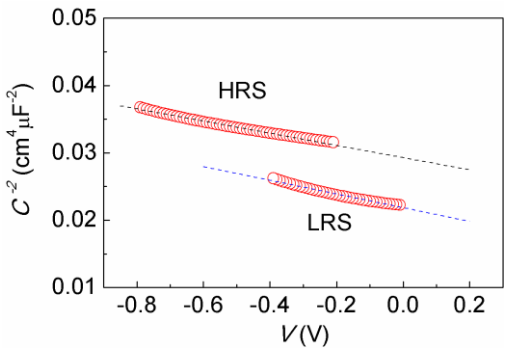

Fig. 4 $1/C^2$- *V* curves of the Ni/Nb:SrTiO$_3$/Ti stack at HRS and LRS. The dotted lines are fitting results.

Now it is clear that LRS and HRS are due to different Schottky barrier heights. To make the relation more visible, the impedance spectroscopy investigations of the Ni/Nb:SrTiO$_3$/Ti stack were conducted again, and the spectra in HRS and LRS are presented in Fig. 5. Immediately after the voltage sweep of 0 → −4 → 0 V, the impedance spectrum at HRS [Fig. 5(a)] was recorded; and after the voltage sweep of 0 → +4 → 0 V, the impedance spectrum at LRS [Fig. 5(b)] was recorded. The diameter of the impedance semi-circle can be regarded as a visual measure of the Schottky barrier; it is obvious from Fig. 5 that HRS is due to a larger Schottky barrier height, and that LRS due to a smaller Schottky barrier height.

In the Schottky contact model, the value of the contact resistance is related to the height of the Schottky barrier and the width of the depletion layer. Considering all the experimental results presented in the above, we come up with a plausible switching mechanism. Different defects (e.g. oxygen vacancies) act as interface states in the interface.[18,30] An interfacial layer inevitably exists on the Ni/Nb:SrTiO$_3$ interface,[28] and forms a potential drop Δ across the interfacial layer. The Schottky barrier height can be written as: $\phi_B = \phi_M - \chi_S - \Delta$. When a forward voltage is applied to the Ni/Nb:SrTiO$_3$ interface, a large amount of electrons are extracted from the interface states, leading to an increase of Δ. This discharge effect decreases the Schottky barrier height and results in LRS.

When a reverse voltage is applied, electrons are trapped in the interface states, and the Schottky barrier height increases, leading to HRS. The amount of trapped/detrapped electrons in the interface states can be modified by controlling the magnitude of voltage or pulse,[28] which induces different Schottky barrier heights, and thus different resistance states are obtained.

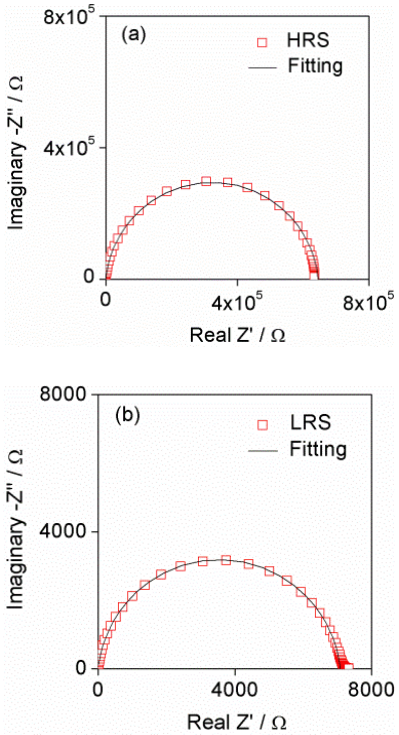

Fig. 5 Impedance spectra of Ni/Nb:$SrTiO_3$/Ti stack in (a) HRS and (b) LRS.

Conclusion

An unambiguous relation between the resistance state and the Schottky barrier height is established, and the impedance spectroscopy investigations make such a relation clearly visible. The variation of Schottky barrier height can be attributed to charge trapping/detrapping in the interface states.

Acknowledgement

This work is supported by the National Natural Science Foundation of China (Grant No. 51372094).

Notes and references

[a] *Laboratory of Solid State Ionics, School of Materials Science and Engineering, Huazhong University of Science and Technology, Wuhan 430074, P. R. China*
**E-mail:xguo@hust.edu.cn*

1 S. Q. Liu, N. J. Wu and A. Ignatiev, *Appl. Phys. Lett.*, 2000, **76**, 2749-2751.
2 X. Chen, N. Wu, J. Strozier and A. Ignatiev, *Appl. Phys. Lett.*, 2006, **89**, 063507.
3 A. Beck, J. G. Bednorz, Ch. Gerber, C. Rossel and D. Widmer, *Appl. Phys. Lett.*, 2000, **77**, 139-141.
4 Z. B. Yan, Y. Y. Guo, G. Q. Zhang and J. M. Liu, *Adv. Mater.*, 2011, **23**, 1351-1355.
5 D. Pantel, S. Goetze, D. Hesse and M. Alexe, *ACS Nano*, 2011, **5,** 6032-6038.
6 Y. Watanabe, J. G. Bednorz, A. Bietsch, Ch. Gerber, D. Widmer, A. Beck and S. J. Wind, *Appl. Phys. Lett.*, 2001, **78**, 3738-3740.
7 T. Fuji, M. Kawasaki, A. Sawa, H. Akoh, Y. Kawazoe and Y. Tokura, *Appl. Phys. Lett.*, 2005, **86**, 012107.
8 D. Choi, D. Lee, H. Sim, M. Chang and H. Hwang, *Appl. Phys. Lett.*, 2006, **88**, 082904.
9 S. Karg, G. I. Meijer, D. Widmer and J. G. Bednorz, *Appl. Phys. Lett.*, 2006, **89**, 072106.
10 K. Szot, W. Speier, G. Bihlmayer and R. Waser, *Nat. Mater.*, 2006, **5**, 312-320.
11 M. Janousch, G. I. Meijer, U. Staub, B. Delley, S. F. Karg and B. P. Andreasson, *Adv. Mater.*, 2007, **19**, 2232-2235.
12 F. La Mattina, J. G. Bednorz, S. F. Alvarado, A. Shengelaya and H. Keller, *Appl. Phys. Lett.*, 2008, **93**, 022102.
13 R. Waser and M. Aono, *Nat. Mater.*, 2007, **6**, 833-840.
14 R. Waser, R. Dittmann, G. Staikov and K. Szot, *Adv. Mater.*, 2009, **21**, 2632-2663.
15 A. Sawa, *Mater. Today*, 2008, **11**, 28-36.
16 X. Guo, *Appl. Phys. Lett.*, 2012, **101**, 152903.
17 Y. Aoki, C. Wiemann, V. Feyer, H. S. Kim, C. M. Schneider, H. I. Yoo and M. Martin, *Nat. Commun.*, 2014, **5**, 3473.
18 A. Sawa, T. Fujii, M. Kawasaki and Y. Tokura, *Proc. SPIE.*, 2005, **5932**, 59322C.
19 T. Menke, P. Meuffels, R. Dittmann, K. Szot and R. Waser, *J. Appl. Phys.*, 2009, **105**, 066104.
20 J. Lee, E. M. Bourim, D. Shin, J. S. Lee, D. J. Seong, J. Park, W. Lee, M. Chang, S. Jung, J. Shin and H. Hwang, *Curr. Appl. Phys.*, 2010, **10**, e68-e70.
21 Y. D. Xia, Z. G. Liu, W. Yang, L. Shi, L. Chen, J. Yin and X. K. Meng, *Appl. Phys. Lett.*, 2007, **91**, 102904.
22 X. L. Jiang, Y. G. Zhao, Y. S. Chen, D. Li, Y. X. Luo, D. Y. Zhao, Z. Sun, J. R. Sun and W. H. Zhao, *Appl. Phys. Lett.*, 2013, **102**, 253507.
23 C. H. Lai and C. Y. Liu, *Appl. Phys. Lett.*, 2013, **103**, 263505.
24 N. T. Ho, V. Senthilkumar and Y. S. Kim, *Solid-State Electronics*, 2014, **94**, 61-65.
25 J. Robertson and C. W. Chen, *Appl. Phys. Lett.*, 1999, **74**, 1168-1170.
26 C. Park, Y. Seo, J. Jung and D. W. Kim, *J. Appl. Phys.*, 2008, **103**, 054106.
27 S. M. Sze and K. K. Ng, *Physics of Semiconductor Devices, 3rd ed.* (Wiley, New Jersey, 2007).
28 E. Mikheev, B. D. Hoskins, D. B. Strukov and S. Stemmer, *Nat. Commun.*, 2014, **5**, 3990.
29 M. C. Ni, S. M. Guo, H. F. Tian, Y. G. Zhao and J. Q. Li, *Appl. Phys. Lett.*, 2014, **91**, 183502.
30 T. Shimizu and H. Okushi, *J. Appl. Phys.*, 1999, **85**, 7244-7251.
31 M. Yang, L. Z. Ren, Y. J. Wang, F. M. Yu, M. Meng, W. Q. Zhou, S. X. Wu and S. W. Li, *J. Appl. Phys.*, 2014, **115**, 134505.
32 Y. Hikita, Y. Kozuka, K. Susaki, H. Takagi and H. Y. Wang, *Appl. Phys. Lett.*, 2007, **90**, 143507.

